UC Irvine

UC Irvine Previously Published Works

Title

T Cell Receptor Signaling Co-regulates Multiple Golgi Genes to Enhance N-Glycan Branching* ♦

Permalink

https://escholarship.org/uc/item/6vk7t807

Journal

Journal of Biological Chemistry, 284(47)

ISSN

0021-9258

Authors

Chen, Hung-Lin
Li, Carey Fei
Grigorian, Ani
et al.

Publication Date

2009-11-01

DOI

10.1074/jbc.m109.023630

Copyright Information

This work is made available under the terms of a Creative Commons Attribution License, availalbe at https://creativecommons.org/licenses/by/4.0/

Peer reviewed

eScholarship.org Powered by the California Digital Library
University of California

THE JOURNAL OF BIOLOGICAL CHEMISTRY VOL. 284, NO. 47, pp. 32454–32461, November 20, 2009
© 2009 by The American Society for Biochemistry and Molecular Biology, Inc. Printed in the U.S.A.

T Cell Receptor Signaling Co-regulates Multiple Golgi Genes to Enhance *N*-Glycan Branching*◆

Received for publication, May 20, 2009, and in revised form, August 13, 2009 Published, JBC Papers in Press, August 25, 2009, DOI 10.1074/jbc.M109.023630

Hung-Lin Chen‡, Carey Fei Li§, Ani Grigorian§, Wenqiang Tian§, and Michael Demetriou‡§1

From the Departments of §Neurology and ‡Microbiology and Molecular Genetics, University of California, Irvine, California 92697

T cell receptor (TCR) signaling enhances β1,6GlcNAc-branching in *N*-glycans, a phenotype that promotes growth arrest and inhibits autoimmunity by increasing surface retention of cytotoxic T lymphocyte antigen-4 (CTLA-4) via interactions with galectins. *N*-Acetylglucosaminyltransferase V (*MGAT5*) mediates β1,6GlcNAc-branching by transferring *N*-acetylglucosamine (GlcNAc) from UDP-GlcNAc to *N*-glycan substrates produced by the sequential action of Golgi α1,2-mannosidase I (MIa,b,c), *MGAT1*, α1,2-mannosidase II (MII, IIx), and *MGAT2*. Here we report that TCR signaling enhances mRNA levels of MIa,b,c and MII,IIx in parallel with *MGAT5*, whereas limiting levels of *MGAT1* and *MGAT2*. Blocking the increase in MI or MII enzyme activity induced by TCR signaling with deoxymannojirimycin or swainsonine, respectively, limits β1,6GlcNAc-branching, suggesting that enhanced MI and MII activity are both required for this phenotype. *MGAT1* and *MGAT2* have an ~250- and ~20-fold higher affinity for UDP-GlcNAc than MGAT5, respectively, and increasing MGAT1 expression paradoxically inhibits β1,6GlcNAc branching by limiting UDP-GlcNAc supply to *MGAT5*, suggesting that restricted changes in *MGAT1* and *MGAT2* mRNA levels in TCR-stimulated cells serves to enhance availability of UDP-GlcNAc to *MGAT5*. Together, these data suggest that TCR signaling differentially regulates multiple *N*-glycan-processing enzymes at the mRNA level to cooperatively promote β1,6GlcNAc branching, and by extension, CTLA-4 surface expression, T cell growth arrest, and self-tolerance.

T cell activation and differentiation induce a number of functionally important changes in cell surface *N*-glycosylation (1–4). For example, activation signaling leads to replacement of α2,6-linked sialic acid with α1,3-linked galactose on the termini of *N*-acetyllactosamine (Galβ1,4GlcNAc) units. *N*-Acetyllactosamine is the ligand for the galectin family of carbohydrate-binding proteins, and the addition of terminal α2,6-linked sialic acid by the ST6Gal1 transferase inhibits galectin binding (4–7). T cell differentiation leads to enhanced expression of ST6Gal1 in T_H2 relative to T_H1/T_H17 cells, thereby reducing sensitivity to galectin-1-induced apoptosis(4). Galectins bind surface glycoproteins in proportion to *N*-acetyllactosamine content, forming a molecular lattice that regulates distribution of glycoproteins to membrane microdomains (*i.e.* lipid rafts) and inhibits their loss to endocytosis(1, 8–13). Binding avidity of galectins for glycoproteins is regulated by the number of attached *N*-glycans (*i.e.* N = occupied N-*X*-(S/T) sites, $X \neq P$), an encoded feature of protein sequences, as well as the degree of Golgi-mediated GlcNAc branching, which together determine *N*-acetyllactosamine content in glycoproteins(14). The number of N-*X*-(S/T) sites varies widely between different glycoproteins, with growth-promoting membrane glycoproteins (*e.g.* T cell receptor (TCR))[2] generally displaying large numbers of N-*X*-(S/T) sites (*i.e.* $n > 5$), whereas growth inhibitory receptors (*e.g.* cytotoxic T lymphocyte antigen-4 (CTLA-4)) have few *N*-glycans ($n \leq 4$)(14). The large difference in galectin avidity for high and low multiplicity receptors allows Golgi-mediated changes in GlcNAc branching to differentially control surface retention (*i.e.* endocytosis rates) of these receptors and therefore transitions between growth and arrest signaling (14).

In resting T cells, where endocytosis is minimal, galectin-3 binds the TCR and the tyrosine phosphatase CD45 but partitions them to different membrane compartments by opposing F-actin targeting (12). Galectin binding prevents spontaneous TCR oligomerization in the absence of antigen, thereby blocking recruitment of multiple adaptor proteins and CD4-Lck to TCR, F-actin-mediated transfer to GM1-enriched lipid microdomains (GEMs), and activation signaling by Lck. In parallel, galectin partitions CD45 to GEMs by counteracting F-actin-mediated exclusion, dampening Lck activation. Upon encounter with antigen, GEMs cluster at the immune synapse formed at the contact site between T cells and antigen-presenting cells, with the galectin lattice reducing TCR/CD4-Lck and increasing CD45 concentration to dampen T cell activation and T_H1 differentiation (1, 2, 12). After activation, membrane turnover increases in T cell blasts, markedly limiting surface levels of the growth inhibitor CTLA-4 via constitutive endocytosis (14). GlcNAc branching increases in blasting T cells, enhancing CTLA-4 affinity for galectins and opposing surface loss to

* This work was supported, in whole or in part, by National Institutes of Health Grants AI053331 and AI082266 (to M. D.) and F32AI081456 (to A. G. and M. D.) through the NIAID and National Institutes of Health Immunology Training Grant T32 AI-060573 (to C. L.).

◆ This article was selected as a Paper of the Week.

[1] To whom correspondence should be addressed: Depts. of Neurology and Microbiology and Molecular Genetics, Institute for Immunology, 250 Sprague Hall, University of California, Irvine, CA 92697. Tel.: 949-824-9775; Fax: 949-824-9847; E-mail: mdemetri@uci.edu.

[2] The abbreviations used are: TCR, T cell receptor; GEM, GM1-enriched lipid microdomains; EAE, experimental autoimmune encephalomyelitis; MI, α-mannosidase I; MII, α-mannosidase II; L-PHA, leukoagglutinin; FITC, fluorescein isothiocyanate; FACS, fluorescence-activated cell sorter; ELISA, enzyme-linked immunosorbent assay; PBMC, peripheral blood mononuclear cell; MBP, myelin basic protein; IL, interleukin; IFN, interferon; SW, swainsonine; DMN, deoxymannojirimycin; MAPK, mitogen-activated protein kinase.

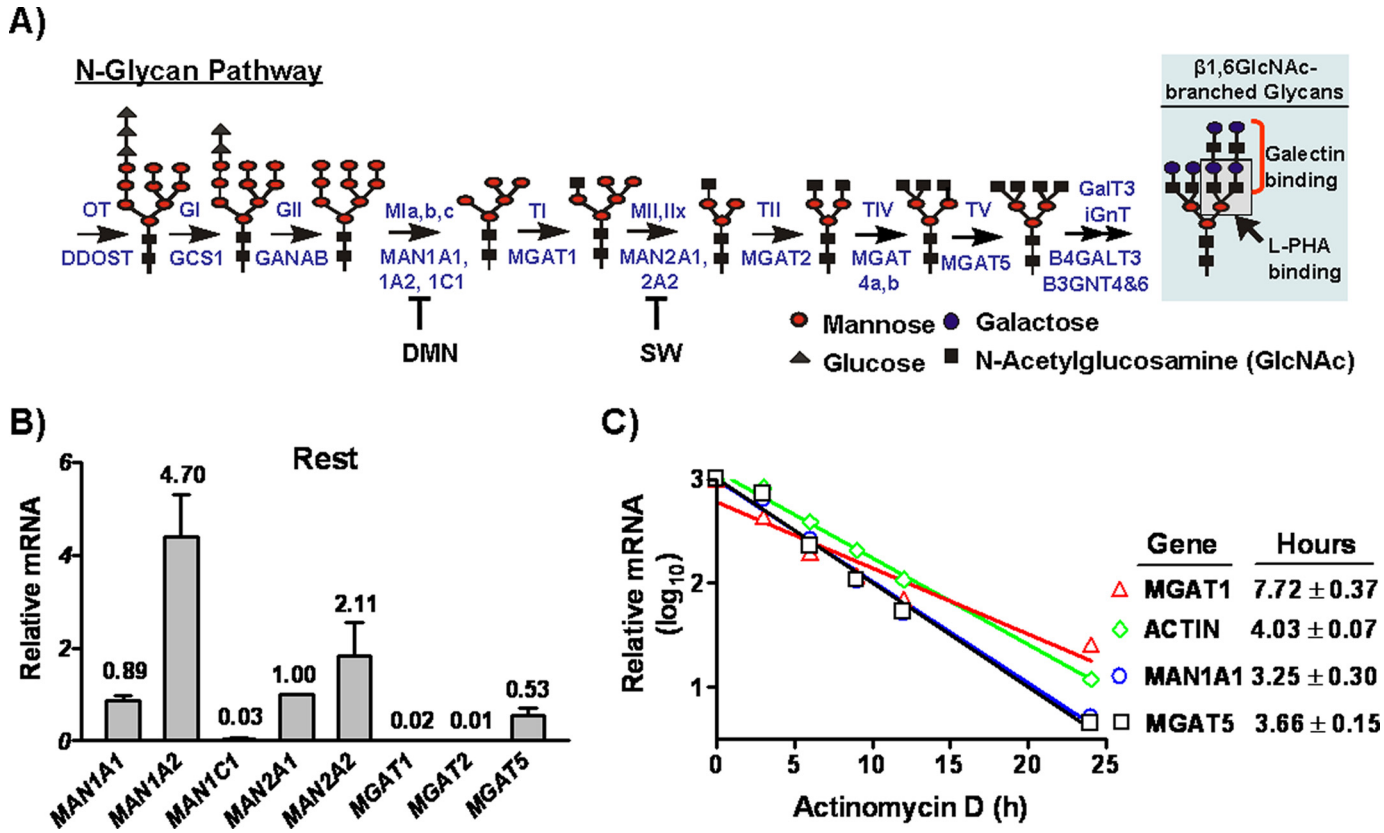

FIGURE 1. **mRNA levels of *N*-glycan GlcNAc branching pathway genes in resting Jurkat T cells.** *A*, *N*-glycosylation pathway in mammals, with enzyme and human gene names above and below the arrows, respectively. *OT/DDOST*, dolichyl-diphosphooligosaccharide-protein glycosyltransferase; *GI/GCS1*, glucosidase I; *GII/GANAB*, glucosidase II; *MIa,b,c/MAN1A1*, *MAN1A2*, *MAN1C1*, α-mannosidase I; *MII,IIx/MAN2A1*, *MAN2A2*, α-mannosidase II; *TI*, *TII*, *TIV*, *TV/MGAT1*, *MGAT2*, *MGAT4a,b*, and *MGAT5*, *N*-acetylglucosaminyltransferases I, II, IV, and V. *B*, relative mRNA expression of *N*-glycan pathway genes in resting Jurkat T cells by TaqMan quantitative real-time PCR, normalized to *MAN2A1*. *Error bars* represent mean ± S.E. of triplicate values. *C*, relative mRNA decay by TaqMan quantitative real-time PCR following the addition of the transcriptional inhibitor actinomycin D to unstimulated Jurkat T cells. mRNA level at 0 h was arbitrarily set at log 3 for all genes. The half-life of each gene was calculated by converting C_t values via a standard curve generated for each primer.

endocytosis (14). Thus, GlcNAc branching in *N*-glycans negatively regulates T cell growth early by raising T cell activation thresholds and later by enhancing CTLA-4-mediated growth arrest.

GlcNAc branching is regulated by activities of the medial Golgi *N*-acetylglucosaminyltransferases I, II, IV, and V (*i.e.* Mgat1, Mgat2, Mgat4, and Mgat5) (15), as well as metabolic supply of their shared substrate UDP-GlcNAc (14, 16). Mgat1, Mgat2, Mgat4, and Mgat5 transfer *N*-acetylglucosamine from UDP-GlcNAc to *N*-glycans transiting the medial Golgi, forming mono-, bi-, tri-, and tetra-antennary GlcNAc-branched *N*-glycans (see Fig. 1*A*). β1,6GlcNAc-branched *N*-glycans produced by Mgat5 are preferentially extended by poly-*N*-acetyllactosamine, generating high affinity ligands for galectins (7, 17). Mgat5-deficient 129/Sv mice display T cell hyperactivity *in vivo*, as exemplified by enhanced type IV hypersensitivity, spontaneous kidney autoimmunity, and increased experimental autoimmune encephalomyelitis (EAE) (1), an animal model of multiple sclerosis. Susceptibility of inbred mouse strains to EAE varies widely and correlates with strain-specific deficiencies in GlcNAc branching in T cells (18). The EAE-susceptible PL/J strain intrinsically possesses reduced basal activities of Mgat1, Mgat2, and Mgat5 and develops a spontaneous multiple sclerosis-like disease that is markedly enhanced by Mgat5$^{+/-}$ and Mgat5$^{-/-}$ backgrounds in a gene dose-dependent manner. Autoimmunity is a complex trait that is influenced by environmental inputs. In this regard, *N*-glycan GlcNAc branching is regulated by the nutrient environment and metabolism via hexosamine pathway production of UDP-GlcNAc, the sugar nucleotide donor for Mgat1, Mgat2, Mgat4, and Mgat5 (14, 16). Overexpression of Mgat1, an enzyme that has an ~250-fold lower K_m for UDP-GlcNAc than Mgat5, paradoxically reduces β1,6GlcNAc branching by limiting UDP-GlcNAc supply to Mgat5 (14). Metabolic supplements to the hexosamine pathway suppress TCR signaling, T cell activation/proliferation, T_H1 differentiation, CTLA-4 endocytosis, and autoimmunity (EAE and autoimmune diabetes). TCR signaling results in sequential increases in glucose flux, UDP-GlcNAc production, β1,6GlcNAc branching, and finally, CTLA-4 surface expression.

These data implicate TCR signaling-mediated enhancement of GlcNAc branching as a critical regulator of CTLA-4 surface retention and autoimmunity. In addition to the Mgat enzymes, Golgi α-mannosidase I (MI) and II (MII) are required for GlcNAc branching (15, 19, 20). MI acts upstream and MII acts downstream of Mgat1, steps required for the action of Mgat2 and production of bi-, tri-, and tetra-antennary *N*-glycans (see Fig. 1*A*). In mammals, the Mgat1, Mgat2, and Mgat5 enzymes are encoded by single genes, whereas three genes encode MI (MIa = *MAN1A1*, MIb = *MAN1A2*, MIc = *MAN1C1*) and two encode MII (*MAN2A1*, *MAN2A2*). In T cells, *MAN2A1* and

MAN2A2 are both expressed, and loss of the former is reported to have little effect on GlcNAc branching or T cell growth (21). Effects of targeted deletion of other Golgi α-mannosidase genes in T cells have not been explored (22, 23). Here we report that TCR signaling enhances expression of all five Golgi α-mannosidase genes in parallel with Mgat5, an activity required for optimal production of β1,6GlcNAc-branched *N*-glycans. In contrast, TCR signaling has little or negative effect on Mgat1 and Mgat2 expression, presumably to increase supply of UDP-GlcNAc to Mgat4 and Mgat5 and promote GlcNAc branching. Our data suggest that TCR signaling differentially regulates multiple Golgi enzymes at the mRNA levels to enhance GlcNAc branching in T cell blasts, and subsequently, growth arrest by CTLA-4.

EXPERIMENTAL PROCEDURES

Cell Culture, FACS, and ELISA—Human Jurkat T cells and peripheral blood mononuclear cells (PBMCs) were cultured in RPMI 1640 medium, supplemented with 10% fetal bovine serum, 2 mM L-glutamine, 100 units/ml penicillin, and 100 μg/ml streptomycin, and 50 μM β-mercaptoethanol. For FACS, cells were collected and stained with fluorescent labeled *Phaseolus vulgaris* leukoagglutinin (L-PHA-FITC, Vector Laboratories) and anti-CD4 antibody as described previously (16). Splenocytes from myelin basic protein (MBP) immunized and non-immunized PL/J mice were stained with anti-CD4 (RM4–5), anti-CD25 (PC61), and anti-CD69 (H1.2F3) from eBioscience and L-PHA-FITC from Vector Laboratories. All incubations and washes were performed on ice. Analyses were done with a FACScan flow cytometer using the CellQuest program (BD Biosciences). ELISA for IL-2 was performed on supernatant from PBMCs stimulated for 2 days as per the manufacturer's instructions (eBioscience).

Quantitative Real-time PCR and mRNA Half-life Measurement—Total mRNA was extracted from Jurkat cells stimulated by 0.5 or 1 μg/ml anti-CD3 (clone OKT3) and anti-CD28 (eBioscience) for 0, 3, 6, 12, 24, 48, and 72 h by the RNeasy® mini kit (Invitrogen). Reverse transcription was performed by the RETROscript® kit (Ambion) according to the manufacturer's instructions. TaqMan probe and primers were purchased from Applied Biosystems, and real-time PCR reactions were performed on the Applied Biosystems 7900HT fast real-time PCR system with the following parameters: 50 °C for 2 min; 95 °C for 10 min; and 40 cycles of 95 °C for 15 s and 60 °C for 1 min. Cycle threshold (C_t) values were determined by the ABI SDS2.1 software. The relative mRNA expression was determined form the cycle threshold (C_t) values using the ABI SDS2.1 software and normalized to actin expression and then to the corresponding mock-treated cells. TaqMan probe and primer sets used were: *MAN1A1*, Hs.00255156_m1; *MAN1A2*, Hs.00198611_m1; *MAN1C1*, Hs.00220595_m1; *MAN2A1*, Hs.00159007_m1; *MAN2A2*, Hs.00196172_m1; *MGAT1*, Hs.00159121_m1; *MGAT2*, Hs.00267183_s1; *MGAT5*, Hs.00159136_m1; IL-2, Hs.00174114_m1; IL-4, Hs.00174122_m1; interferon-γ (IFNγ), Hs.00174143_m1; β-actin, Hs.9999903_m1.

To measure mRNA stability, cDNA was derived from cells treated for 0, 3, 6, 9, and 12 h with the transcriptional inhibitor actinomycin D (5 μg/ml, Sigma). C_t values were compared with mock-treated cells at corresponding time points, with mRNA half-life determined using a standard curve generated by 2-fold serial dilutions for each primer (24).

Phylogenetic Analysis—10 kb of 5′-untranslated region upstream sequences for various *N*-glycan-processing genes were

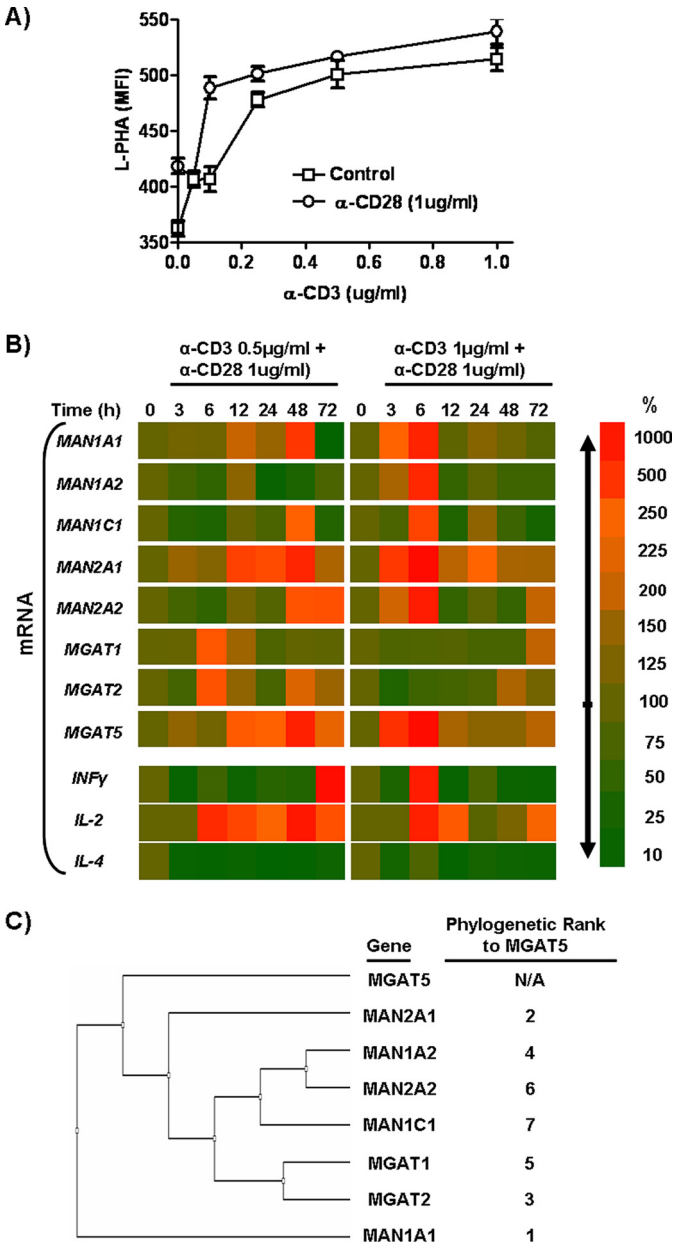

FIGURE 2. **mRNA levels of *N*-glycan pathway genes in activated Jurkat T cells.** *A*, flow cytometry analysis of Jurkat T cells stained with L-PHA-FITC, a marker of GlcNAc branching in *N*-glycans, following stimulation with soluble anti-CD3 (OKT3) and co-stimulatory soluble anti-CD28 for 72 h; *MFI*, mean fluorescence intensity. *Error bars* represent mean ± S.E. of triplicate values. *B*, quantitative real-time PCR of *N*-glycan pathway (*MAN1A1*, *MAN1A2*, *MAN1C1*, *MAN2A1*, *MAN2A2*, *MGAT1*, *MAGT2*, and *MGAT5*) and cytokine (IFNγ, IL-2, and IL-4) genes in Jurkat T cells stimulated with soluble anti-CD3 + soluble anti-CD28 (1 μg/ml). The -fold difference was calculated by the $\Delta\Delta C_t$ method using glyceraldehyde-3-phosphate dehydrogenase as an endogenous control, with colorimetric results displaying comparisons with unstimulated mock control cells at each time point (*i.e.* 0, 3, 6, 9, 12, 24, 48, and 72 h). *C*, 10 kb of 5′-untranslated region nucleotide sequences of *N*-glycan pathway genes were retrieved from the Geneatlas data base and analyzed by the BioEdit software. The phylogenetic graph and distance were generated by the Neighbor-Joining/UPGMA method Version 3.62a2.1. *N/A*, not applicable.

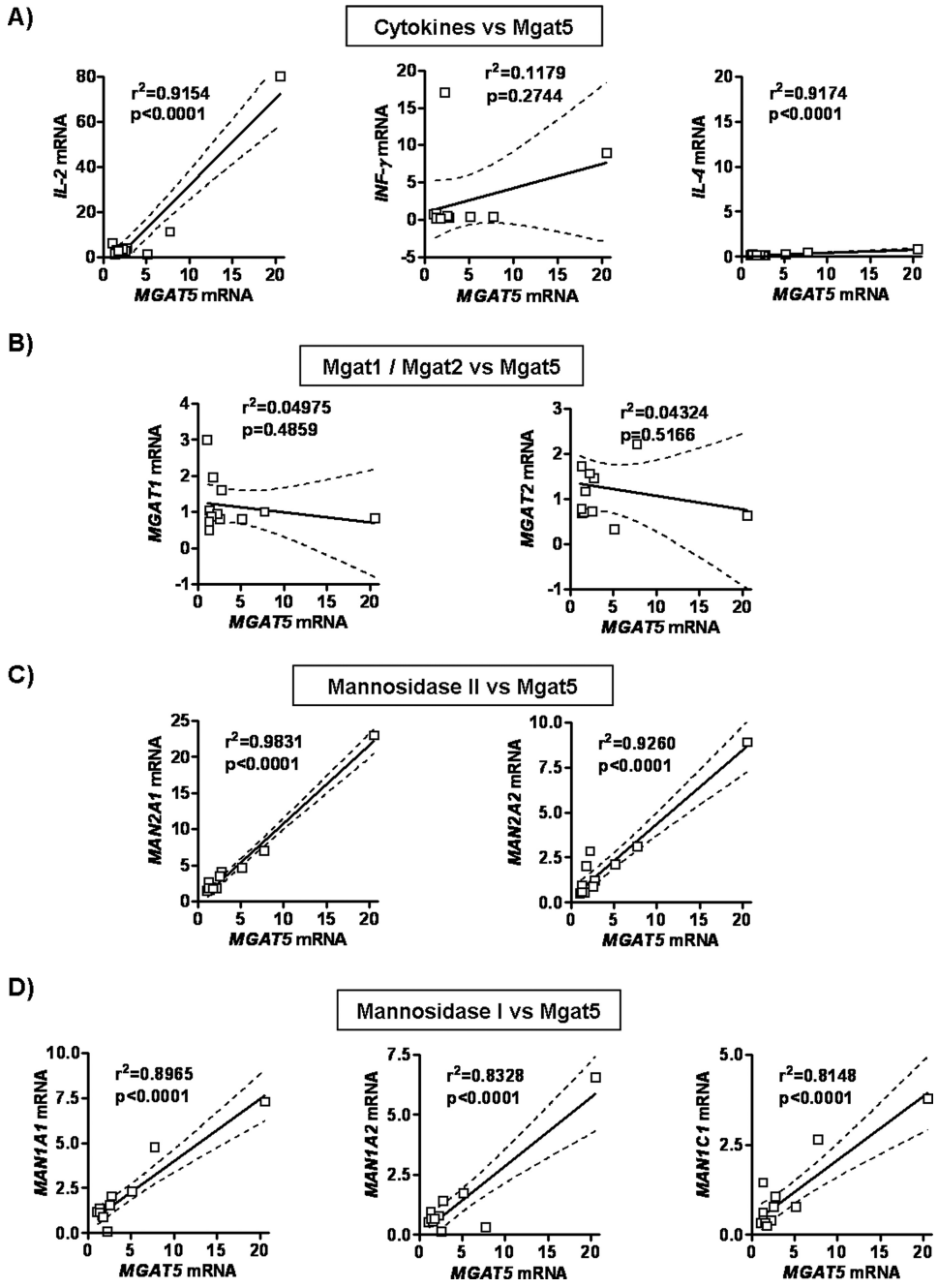

FIGURE 3. **mRNA correlation of *MGAT5* with *N*-glycan and cytokine genes following TCR activation.** *A–D*, expression data from Fig. 2*B* (both 0.5 μg/ml and 1 μg/ml anti-CD3-stimulated cells) were plotted to compare *MGAT5* with cytokines (IL-2, IL-4, and INF-γ) (*A*), *MGAT1* and *MGAT2* (*B*), mannosidase II (*MAN2A1* and *MAN2A2*) (*C*), and mannosidase I (*MAN1A1*, *MAN1A2*, and *MAN1C1*) (*D*). The correlation coefficient R^2, *p* value, and 95% confidence intervals (*dotted line*) were calculated by the Prism software.

retrieved from the Geneatlas data base and phylogenetically analyzed using the Neighbor-Joining/UPGMA (unweighted pair group method with arithmetic mean) method (Version 3.62a2.1) (25). A phylogenetic distance value relative to *MGAT5* generated by this software is also reported in Fig. 2*C*.

EAE Model of Inflammatory, Autoimmune Disease—EAE was induced by subcutaneous immunization of wild-type PL/J mice on days 0 and 15 with 100 μg of bovine MBP (Sigma) emulsified in complete Freund's adjuvant containing 4 mg/ml heat-inactivated *Mycobacterium tuberculosis* (H37RA; Difco) distributed over two spots on the hind flank. Splenocytes were harvested at day 40 and analyzed by FACS. All procedures and protocols with mice were approved by the Institutional Animal Care and Use Committee of the University of California, Irvine, CA.

RESULTS

Basal mRNA Levels of N-Glycan Pathway Genes in Jurkat T Cells—We assessed relative mRNA levels of multiple *N*-glycan pathway genes in resting Jurkat T cells by TaqMan quantitative real-time PCR. We examined MI genes (*MAN1A1*, *MAN1A2*, and *MAN1C1*), MII genes (*MAN2A1* and *MAN2A2*), and *MGAT1*, *MGAT2*, and *MGAT5* (Fig. 1*A*). Basal mRNA levels of *MAN1C1*, *MGAT1*, and *MGAT2* were ~25–500-fold lower than the other tested genes (Fig. 1*B*). MI is encoded by three genes, and these data suggest that *MAN1A1* and *MAN1A2* are the major contributors to MI enzyme activity in Jurkat T cells. In contrast, *MGAT1* and *MGAT2* are the only genes encoding *N*-acetylglucosaminyltransferases I and II, respectively, and are absolutely required for GlcNAc branching (26–28). Monitoring the decay of mRNA by quantitative real-time PCR in Jurkat T cells treated with the transcriptional inhibitor actinomycin D (24) suggests that the mRNA half-life of *MGAT1* ($t_{1/2}$ = 7.7 h) is approximately twice that of *MGAT5* ($t_{1/2}$ = 3.7 h), *MAN1A1* ($t_{1/2}$ = 3.3 h), and actin ($t_{1/2}$ = 4.0 h) (Fig. 1*C*). This suggests that the large difference in mRNA levels of *MGAT1 versus MGAT5* arises predominantly from differences in transcriptional control rather than mRNA stability.

TCR Signaling Differentially Regulates MGAT5 versus MGAT1 and MGAT2 mRNA—GlcNAc branching is significantly enhanced by TCR signaling, a phenotype that limits cell surface loss of CTLA-4 by endocytosis (1, 2, 14). FACS analysis with leukoagglutinin (L-PHA), a plant lectin recognizing β1,6GlcNAc-branched *N*-glycans produced by Mgat5, provides a useful marker of cell surface GlcNAc branching (29). Consistent with previous observations in mouse *ex vivo* T cells (1, 2), L-PHA binding and *MGAT5* mRNA levels in Jurkat T cells increase in proportion to TCR signal strength induced by

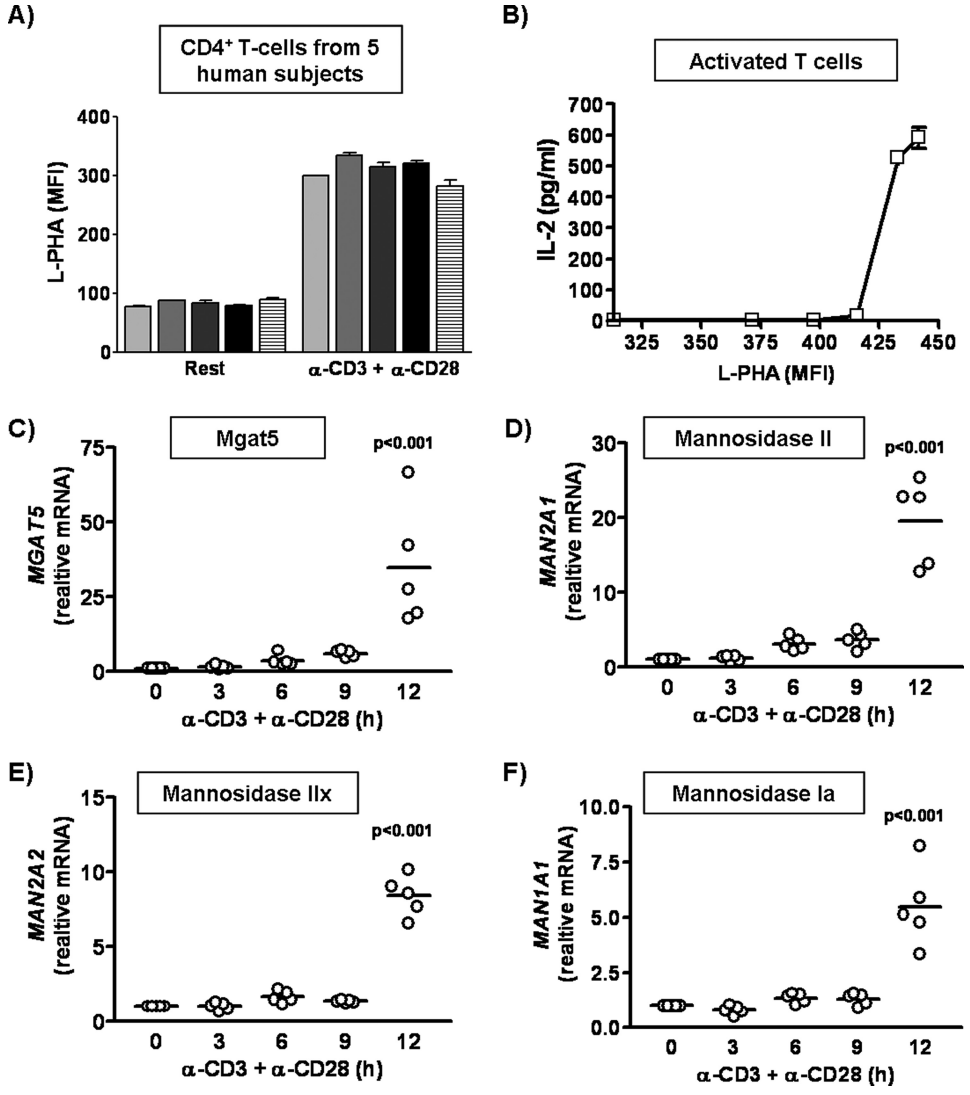

FIGURE 4. ***N*-Glycan branching and mRNA levels of Golgi genes in TCR activated human T cells.** *A* and *C–F*, PBMCs from five healthy human control subjects at rest or stimulated with either 1 μg/ml soluble anti-CD3 or 1 μg/ml soluble anti-CD28 were analyzed for L-PHA binding at 72 h by flow cytometry (*A*) and mRNA levels of the indicated genes at 3, 6, 9, and 12 h by TaqMan quantitative real-time PCR (*C–F*) as described in the legend for Fig. 2. Cells in *A* are gated on the $CD4^+$ population. *p* values in *C–E* were determined by one-way analysis of variance and Neuman-Keuls multiple comparison test (only *p* values < 0.05 are shown). *MFI*, mean fluorescence intensity. *B*, PBMCs were stimulated for 48 h with increasing amounts of plate-bound anti-CD3 antibody (1, 2, 4, 8, 16, and 32 ng/ml) + 2 μg/ml soluble anti-CD28. L-PHA binding in $CD4^+$ T cells and IL-2 levels in the supernatant were measured by FACS and ELISA, respectively. *Error bars* represent mean ± S.E. of triplicate values.

anti-CD3 antibody (Fig. 2, *A* and *B*). The addition of anti-CD28 antibody, which provides a co-stimulatory signal that maximizes T cell activation, further enhanced L-PHA binding (Fig. 2*A*). The expression of *MGAT5* mRNA is regulated by the RAS-RAF-MAPK signaling pathway (30, 31), which is activated by TCR signaling. At lower levels of anti-CD3 stimulation, *MGAT5* mRNA expression is up-regulated ~3-fold starting from 12 h and reaches ~8-fold after 48 h. Notably, stronger anti-CD3 stimulation shifts peak expression to earlier time points (Fig. 2*B*) followed by relatively rapid decline to near baseline. *MGAT5* mRNA has a short half-life (~3.7 h, Fig. 1*C*), suggesting that strong TCR signaling induces a rapid up- and down-regulation of *MGAT5* transcription. Similar kinetics were observed for TCR signaling-mediated changes in IL-2 mRNA, and to a lesser extent, IFNγ (Fig. 2*B*). A correlation plot comparing all time points at both levels of anti-CD3 stimulation revealed a strong statistical correlation between *MGAT5* and IL-2 ($R^2 = 0.915$, $p < 0.0001$, Fig. 3*A*) but not IFNγ ($R^2 = 0.118$, $p = 0.27$, Fig. 3*A*). In contrast, IL-4 mRNA levels were reduced at all time points, including when MGAT5 levels were maximally enhanced by TCR signaling (Fig. 2*B*). However, peak levels of *MGAT5* mRNA were associated with the smallest declines in IL-4 mRNA and *vice versa*; therefore a strong correlation was still observed between these two genes ($R^2 = 0.917$, $p < 0.0001$, Fig. 3*A*).

MGAT1 and *MGAT2* mRNA levels displayed limited increases at low levels of TCR signaling with enhancement occurring significantly earlier than *MGAT5* (Fig. 2*B*). Remarkably, high levels of stimulation reduced *MGAT1* and *MGAT2* mRNA levels by up to ~2-fold at time points when *MGAT5* levels were enhanced (Fig. 2*B*). Indeed, there was no correlation between mRNA levels of *MGAT5* and *MGAT1* or *MGAT2* (Fig. 3*B*). Phylogenic comparison of the 5′ 10-kb promoter regions suggested that the distance between *MGAT5* and *MGAT1* or *MGAT2* (Fig. 2*C*) is consistent with RAS-RAF-MAPK responsiveness of *MGAT5* (30, 31) and predominantly "housekeeping" promoter elements in *MGAT1* and *MGAT2* (32, 33).

TCR Signaling Up-regulates MI and MII in Parallel with MGAT5 to Promote GlcNAc Branching—In contrast to *MGAT1* and *MGAT2,* mRNA levels of the three MI genes (*MAN1A1*, *MAN1A2*, and *MAN1C1*) and two MII genes (*MAN2A1* and *MAN2A2*) increased in parallel with *MGAT5* at both low and high levels of anti-CD3 stimulation (Fig. 2*B*). Statistical analysis of mRNA levels under both conditions showed that the expression levels of *MGAT5* transcripts strongly correlated with *MAN2A1* ($R^2 = 0.9260$, $p < 0.0001$), *MAN2A2* ($R^2 = 0.9260$, $p < 0.0001$), *MAN1A1* ($R^2 = 0.8965$, $p < 0.0001$), *MAN1A2* ($R^2 = 0.8328$, $p < 0.0001$), and *MAN1C1* ($R^2 = 0.8148$, $p < 0.0001$) (Fig. 3, *C* and *D*). At high dose TCR stimulation, peak levels of these genes coincided with down-regulation of *MGAT1* and *MGAT2* mRNA levels (Fig. 2*B*). Phylogenetic analysis of 10 kb upstream of the transcription start site revealed the greatest similarity to *MGAT5* was *MAN2A1* and *MAN1A1* (Fig. 2*C*).

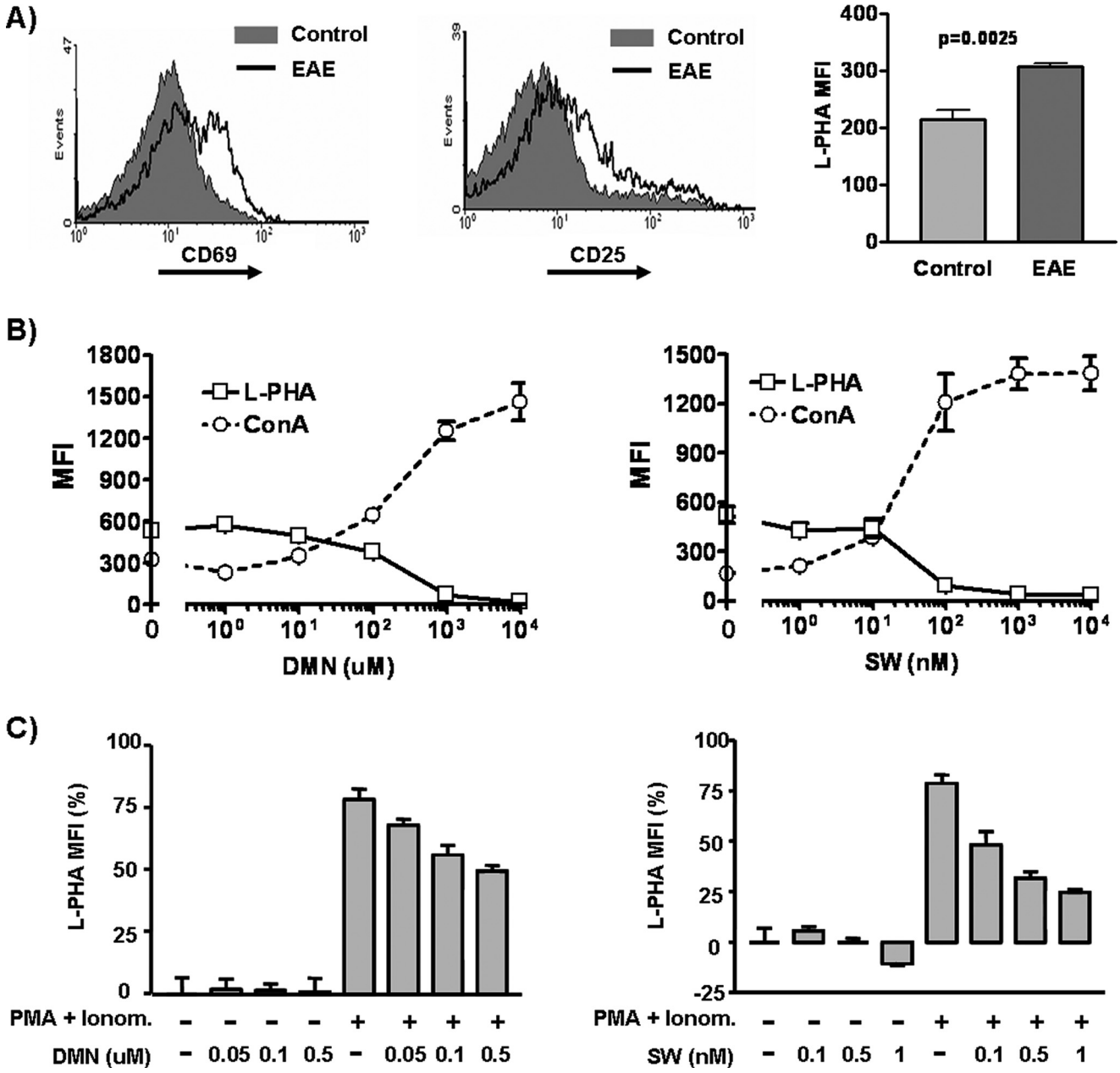

FIGURE 5. **TCR signaling-mediated enhancement of mannosidase I and mannosidase II enzyme activity increases *N*-glycan GlcNAc branching in Jurkat T cells.** *A*, splenocytes from a non-immunized control mouse and a mouse with EAE (clinical score = 2) induced by immunization with MBP + CFA were analyzed by flow cytometry for T cell activation markers (CD69 and CD25) and L-PHA binding (stained in triplicate). Cells are gated on the $CD4^+$ population. *MFI*, mean fluorescence intensity. *Error bars* represent mean ± S.E. of triplicate values. *p* values were determined by Student's *t* test. *B*, flow cytometry analysis of concanavalin A-FITC (*ConA*)- and L-PHA-FITC-stained resting Jurkat T cells treated with increasing concentrations of a mannosidase I or mannosidase II inhibitor for 72 h. Concanavalin A-FITC binds high mannose *N*-glycans, whereas L-PHA binds β1,6GlcNAc-branched *N*-glycans. *C*, Jurkat T cells were stimulated with phorbol 12-myristate 13-acetate (*PMA*) and ionomycin (*Ionom.*) in the presence or absence of minimal concentrations of DMN or SW and analyzed by L-PHA-FITC flow cytometry. The low DMN and SW concentrations were chosen because they have little or no effect on L-PHA binding in unstimulated Jurkat T cells.

Analysis of PBMCs from five healthy human subjects revealed similar results. Anti-CD3 + anti-CD28 stimulation similarly enhanced L-PHA binding in $CD4^+$ T cells from all five subjects (Fig. 4*A*) and correlated with IL-2 secretion (Fig. 4*B*). This was associated with peak increases in mRNA of *MGAT5*, *MAN2A1*, *MAN2A2*, and *MAN1A1* at 12 h after stimulation (Fig. 4, *C–F*). To confirm that T cell activation *in vivo* was associated with increased GlcNAc branching, we compared *ex vivo* mouse T cells from a control mouse with a mouse clinically affected by EAE (an animal model for the human inflammatory disease multiple sclerosis). As expected, FACS analysis of EAE splenocytes revealed increased expression of the T cell activation markers CD69 and CD25 as well as increased L-PHA binding in $CD4^+$ T cells (Fig. 5*A*).

Together, these data suggest that the Mgat5 and Golgi α-mannosidase enzymes are synchronously up-regulated at the transcriptional level by TCR signaling to enhance GlcNAc branching in activated T cells. To confirm that increases in MI and MII enzyme activity are required for up-regulation of GlcNAc branching, we utilized the MI inhibitor deoxymannojiri-

mycin (DMN) and the MII inhibitor swainsonine (SW) (Fig. 1*A*) (34). As expected, co-incubation of non-stimulated Jurkat T cells with increasing concentrations of DMN or SW both markedly reduced GlcNAc branching, as measured by L-PHA, while concurrently increasing high mannose structures, as revealed by concanavalin A staining (Fig. 5*B*). Remarkably, incubation of activated Jurkat T cells with concentrations of DMN and SW that have no effect on L-PHA binding in resting cells prevented phorbol 12-myristate 13-acetate (*PMA*)/ionomycin (*Ionom*)-mediated increases in L-PHA binding (Fig. 5*C*). The minimal concentrations of DMN and SW appear to block the increase in MI and MII activity induced by activation signaling, thereby preventing increased flux of *N*-glycan acceptors to Mgat5 and enhanced β1,6GlcNAc-branched *N*-glycans.

DISCUSSION

GlcNAc branching of *N*-glycans attached to cell surface glycoproteins such as TCR, CD45, and CTLA-4 titrates binding to galectins, forming a molecular lattice that negatively regulates T cell growth and susceptibility to autoimmunity. TCR signaling up-regulates *MGAT5* gene expression and metabolic supply of UDP-GlcNAc to the Golgi to promote GlcNAc branching and CTLA-4 retention at the cell surface. Here we find that TCR signaling differentially regulates mRNA expression of multiple genes upstream of Mgat5 in the Golgi to enhance GlcNAc branching. *MGAT5* mRNA expression strongly correlates with the three Golgi MI and the two Golgi MII genes. Limiting TCR signaling-mediated increases in MI or MII enzyme activity confirms that this phenotype is required to enhance GlcNAc branching. In contrast, TCR signaling-mediated changes in mRNA levels in *MGAT1* and *MGAT2* do not correlate with *MGAT5/MI/MII* genes, being reduced when *MGAT5* expression is maximally increased. *MAGT1*, *MAGT2*, and *MAGT5* act sequentially, utilize UDP-GlcNAc as substrate, and are absolutely required for biosynthesis of β1,6GlcNAc-branched *N*-glycans. However, *MGAT1* and *MGAT2* have 200- and 20-fold lower K_m for UDP-GlcNAc than *MGAT5*, suggesting unequal competition for substrate in the medial Golgi (14). Indeed, overexpression of *MGAT1* reduces GlcNAc branching by reducing supply of UDP-GlcNAc to downstream GlcNAc transferases (14). We conclude that positive regulation of GlcNAc-branched *N*-glycans by TCR signaling, and by extension, CTLA-4 surface retention and inhibition of autoimmunity, require coordinated up-regulation of MI, MII, and Mgat5 activities and UDP-GlcNAc biosynthesis, coupled with limited changes/suppression of Mgat1 and Mgat2.

MAN2A1-deficient resting T cells from C57BL/6 mice are reported to display little change in GlcNAc-branched *N*-glycans, suggesting that *MAN2A2* supplies sufficient MII activity to compensate for this loss (21). Whether this is also true in activated T cells requires further investigation; however, it is consistent with our conclusion that up-regulation of total MII activity, via increases in both *MAN2A1* and *MAN2A2* mRNA, is the physiologically relevant change. Similarly, experimentally blocking up-regulation of a single MI gene in activated T cells is unlikely to be biologically significant; rather, enhanced MI activity distributed over increases in the three genes is likely the relevant phenotype required to increase GlcNAc branching in activated T cells.

Enhanced GlcNAc branching in activated T cells promotes cell surface retention of CTLA-4 (14), a critical negative regulator of autoimmunity (35). Coordinated up-regulation of *MGAT5*, *MAN1A1*, *MAN1A2*, *MAN1C1*, *MAN2A1*, and *MAN2A2* mRNA downstream of TCR signaling suggests a common transcriptional regulator(s) activated by the phosphatidylinositol 3-kinase/ERK pathway. Defining the molecular mechanism for this co-regulation should provide new critical regulators of GlcNAc branching and expand the hexosamine/Golgi gene network regulating CTLA-4 surface retention. Genetic variations in network genes are prime candidates for regulation of human autoimmunity.

Increasing the expression of *MGAT1* reduces GlcNAc branching by reducing availability of UDP-GlcNAc to Mgat4 and Mgat5, suggesting that limiting Mgat1 activity is necessary for optimal increases in GlcNAc branching. *MGAT1* and *MGAT2* are simple genes with two and one exons, respectively, whereas *MGAT5* has 16 exons with long intervening introns. It is tempting to speculate that these differences evolved to permit continuous and consistent production of glycoproteins with a minimum affinity for galectin (*i.e.* mono- and biantennary *N*-glycans by Mgat1 and Mgat2) and limited but tightly regulated production of high affinity galectin ligands by Mgat5. As exemplified in T cells, our data suggest that coordinated expression of multiple *N*-glycan pathway genes and UDP-GlcNAc production by phosphatidylinositol 3-kinase/ERK signaling is necessary for optimal regulation of GlcNAc branching, and when disturbed, may lead to diseases such as autoimmunity, cancer, and type 2 diabetes (1, 36–38).

REFERENCES

1. Demetriou, M., Granovsky, M., Quaggin, S., and Dennis, J. W. (2001) *Nature* **409,** 733–739
2. Morgan, R., Gao, G., Pawling, J., Dennis, J. W., Demetriou, M., and Li, B. (2004) *J. Immunol.* **173,** 7200–7208
3. Comelli, E. M., Sutton-Smith, M., Yan, Q., Amado, M., Panico, M., Gilmartin, T., Whisenant, T., Lanigan, C. M., Head, S. R., Goldberg, D., Morris, H. R., Dell, A., and Paulson, J. C. (2006) *J. Immunol.* **177,** 2431–2440
4. Toscano, M. A., Bianco, G. A., Ilarregui, J. M., Croci, D. O., Correale, J., Hernandez, J. D., Zwirner, N. W., Poirier, F., Riley, E. M., Baum, L. G., and Rabinovich, G. A. (2007) *Nat. Immunol.* **8,** 825–834
5. Amano, M., Galvan, M., He, J., and Baum, L. G. (2003) *J. Biol. Chem.* **278,** 7469–7475
6. Stowell, S. R., Arthur, C. M., Mehta, P., Slanina, K. A., Blixt, O., Leffler, H., Smith, D. F., and Cummings, R. D. (2008) *J. Biol. Chem.* **283,** 10109–10123
7. Hirabayashi, J., Hashidate, T., Arata, Y., Nishi, N., Nakamura, T., Hirashima, M., Urashima, T., Oka, T., Futai, M., Muller, W. E., Yagi, F., and Kasai, K. (2002) *Biochim. Biophys. Acta* **1572,** 232–254
8. Partridge, E. A., Le Roy, C., Di Guglielmo, G. M., Pawling, J., Cheung, P., Granovsky, M., Nabi, I. R., Wrana, J. L., and Dennis, J. W. (2004) *Science* **306,** 120–124
9. Nieminen, J., Kuno, A., Hirabayashi, J., and Sato, S. (2007) *J. Biol. Chem.* **282,** 1374–1383
10. Brewer, C. F., Miceli, M. C., and Baum, L. G. (2002) *Curr. Opin. Struct. Biol.* **12,** 616–623
11. Ahmad, N., Gabius, H. J., André, S., Kaltner, H., Sabesan, S., Roy, R., Liu, B., Macaluso, F., and Brewer, C. F. (2004) *J. Biol. Chem.* **279,** 10841–10847
12. Chen, I. J., Chen, H. L., and Demetriou, M. (2007) *J. Biol. Chem.* **282,** 35361–35372

13. Grigorian, A., Torossian, S., and Demetriou, M. (2009) *Immunol. Rev.* **230,** 232–246
14. Lau, K. S., Partridge, E. A., Grigorian, A., Silvescu, C. I., Reinhold, V. N., Demetriou, M., and Dennis, J. W. (2007) *Cell* **129,** 123–134
15. Schachter, H. (1991) *Glycobiology* **1,** 453–461
16. Grigorian, A., Lee, S. U., Tian, W., Chen, I. J., Gao, G., Mendelsohn, R., Dennis, J. W., and Demetriou, M. (2007) *J. Biol. Chem.* **282,** 20027–20035
17. Cummings, R. D., and Kornfeld, S. (1984) *J. Biol. Chem.* **259,** 6253–6260
18. Lee, S. U., Grigorian, A., Pawling, J., Chen, I. J., Gao, G., Mozaffar, T., McKerlie, C., and Demetriou, M. (2007) *J. Biol. Chem.* **282,** 33725–33734
19. Akama, T. O., Nakagawa, H., Wong, N. K., Sutton-Smith, M., Dell, A., Morris, H. R., Nakayama, J., Nishimura, S., Pai, A., Moremen, K. W., Marth, J. D., and Fukuda, M. N. (2006) *Proc. Natl. Acad. Sci. U.S.A.* **103,** 8983–8988
20. Herscovics, A. (2001) *Biochimie* **83,** 757–762
21. Chui, D., Sellakumar, G., Green, R., Sutton-Smith, M., McQuistan, T., Marek, K., Morris, H., Dell, A., and Marth, J. (2001) *Proc. Natl. Acad. Sci. U.S.A.* **98,** 1142–1147
22. Tremblay, L. O., Nagy Kovács, E., Daniels, E., Wong, N. K., Sutton-Smith, M., Morris, H. R., Dell, A., Marcinkiewicz, E., Seidah, N. G., McKerlie, C., and Herscovics, A. (2007) *J. Biol. Chem.* **282,** 2558–2566
23. Akama, T. O., Nakagawa, H., Sugihara, K., Narisawa, S., Ohyama, C., Nishimura, S., O'Brien, D. A., Moremen, K. W., Millan, J. L., and Fukuda, M. N. (2002) *Science* **295,** 124–127
24. Leclerc, G. J., Leclerc, G. M., and Barredo, J. C. (2002) *Cancer Cell Int.* **2,** 1
25. Saitou, N., and Nei, M. (1987) *Mol. Biol. Evol.* **4,** 406–425
26. Ioffe, E., and Stanley, P. (1994) *Proc. Natl. Acad. Sci. U.S.A.* **91,** 728–732
27. Metzler, M., Gertz, A., Sarkar, M., Schachter, H., Schrader, J. W., and Marth, J. D. (1994) *EMBO J.* **13,** 2056–2065
28. Wang, Y., Tan, J., Sutton-Smith, M., Ditto, D., Panico, M., Campbell, R. M., Varki, N. M., Long, J. M., Jaeken, J., Levinson, S. R., Wynshaw-Boris, A., Morris, H. R., Le, D., Dell, A., Schachter, H., and Marth, J. D. (2001) *Glycobiology* **11,** 1051–1070
29. Cummings, R. D., and Kornfeld, S. (1982) *J. Biol. Chem.* **257,** 11230–11234
30. Buckhaults, P., Chen, L., Fregien, N., and Pierce, M. (1997) *J. Biol. Chem.* **272,** 19575–19581
31. Ko, J. H., Miyoshi, E., Noda, K., Ekuni, A., Kang, R., Ikeda, Y., and Taniguchi, N. (1999) *J. Biol. Chem.* **274,** 22941–22948
32. Yip, B., Chen, S. H., Mulder, H., Höppener, J. W., and Schachter, H. (1997) *Biochem. J.* **321,** 465–474
33. Bendiak, B., and Schachter, H. (1987) *J. Biol. Chem.* **262,** 5784–5790
34. Elbein, A. D. (1987) *Annu. Rev. Biochem.* **56,** 497–534
35. Waterhouse, P., Penninger, J. M., Timms, E., Wakeham, A., Shahinian, A., Lee, K. P., Thompson, C. B., Griesser, H., and Mak, T. W. (1995) *Science* **270,** 985–988
36. Demetriou, M., Nabi, I. R., Coppolino, M., Dedhar, S., and Dennis, J. W. (1995) *J. Cell Biol.* **130,** 383–392
37. Granovsky, M., Fata, J., Pawling, J., Muller, W. J., Khokha, R., and Dennis, J. W. (2000) *Nat. Med.* **6,** 306–312
38. Ohtsubo, K., Takamatsu, S., Minowa, M. T., Yoshida, A., Takeuchi, M., and Marth, J. D. (2005) *Cell* **123,** 1307–1321